

Early Reionization by the First Galaxies

B. Ciardi¹, A. Ferrara² & S. D. M. White¹

¹ *Max-Planck-Institut für Astrophysik, 85741 Garching, Germany*

² *SISSA/International School for Advanced Studies, Via Beirut 4, 34014 Trieste, Italy*

29 October 2018

ABSTRACT

Large-scale polarization of the cosmic microwave background measured by the *WMAP* satellite requires a mean optical depth to Thomson scattering, $\tau_e \sim 0.17$. The reionization of the universe must therefore have begun at relatively high redshift. We have studied the reionization process using supercomputer simulations of a large and representative region of a universe which has cosmological parameters consistent with the *WMAP* results. Our simulations follow both the radiative transfer of ionizing photons and the formation and evolution of the galaxy population which produces them. A previously published model with a standard stellar IMF, with a moderate photon escape fraction from galaxies and with ionizing photon production as expected for zero metallicity stars produces $\tau_e = 0.104$, which is within 1.0 to 1.5σ of the “best” *WMAP* value. Values up to 0.16 can be produced by taking larger escape fractions or a top heavy IMF. The data do not require a separate populations of “miniquasars” or of stars forming in objects with total masses below $10^9 M_\odot$. Reconciling such early reionization with the observed Gunn-Peterson troughs in $z > 6$ quasars may be challenging. Possible resolutions of this problem are discussed.

Key words: galaxies: formation - cosmology: theory - large-scale structure - cosmology: observations

1 MOTIVATION

It has recently become possible to study the reionization of the universe in some detail. Massive numerical computations can now follow not only the clustering of dark matter and gas, but also the formation of galaxies and the propagation of ionizing photons in a highly inhomogeneous, partially ionized, intergalactic medium (IGM). In spite of many poorly understood details concerning the physics of star formation, and the approximations inherent in the various numerical treatments of radiative transfer (for a recent review see Maselli, Ferrara & Ciardi 2003), a number of independent studies have converged on a relatively late ($z_r \lesssim 8$ to 10) epoch for complete reionization of the IGM within current “concordance” (i.e. flat, Λ -dominated) cosmological models (e.g. Ciardi et al. 2000, hereafter CFGJ; Gnedin 2000; Razoumov et al. 2002; Ciardi, Stoehr & White 2003, hereafter CSW).

This conclusion appears challenged by results from the *WMAP* satellite (Kogut et al. 2003; Spergel et al. 2003). This experiment has detected an excess in the CMB TE cross-power spectrum on large angular scales ($\ell < 7$) indicating an optical depth to the CMB last scattering surface of $\tau_e = 0.16$. The uncertainty quoted for this number depends on the analysis technique employed. Fitting the TE

cross power spectrum to Λ CDM models in which all parameters except τ_e take their best fit values based on the TT power spectrum, Kogut et al. (2003) obtain a 68% confidence range, $0.13 < \tau_e < 0.21$. Fitting all parameters simultaneously to the TT+TE data, Spergel et al. (2003) obtain $0.095 < \tau_e < 0.24$. Including additional data external to *WMAP*, these authors were able to shrink their confidence interval to $0.11 < \tau_e < 0.23$. Finally, by assuming that the *observed* TT power spectrum is scattered to produce the *observed* TE cross-power spectrum Kogut et al. (2003) infer $0.12 < \tau_e < 0.20$. It is unclear which of these uncertainty estimates to prefer. Most τ_e values in these ranges require a substantial fraction of the universe to be ionized before redshift 10. For example, $0.12 < \tau_e < 0.20$ translates into $13 < z_r < 19$ in a model where reionization is instantaneous.

Apparently, reionization occurred earlier than expected. Is this discrepancy real? In practice, recovering the “reionization epoch” is subject to some ambiguity related to the specific reionization history assumed (see e.g. Bruscoli, Scannapieco & Ferrara 2002). What might reionization models have overlooked? The discrepancy is not dependent on the particular cosmological parameters adopted, since *WMAP* has confirmed the previous concordance model. Hence the “oversight” must be of astrophysical nature. Several effects might have produced rapid early evolution: a contribution

arXiv:astro-ph/0302451v2 22 Feb 2003

from low-mass pregalactic systems (in the jargon, Population III objects); unexpectedly high star formation efficiency; unexpectedly high ionizing photon production; an unexpectedly large probability for ionizing photons to escape into the IGM; a possible population of early “miniquasars”. In this paper, we point out that efficient production and escape of ionizing photons is sufficient to account for the data within conventional galaxy formation models. The data do not *require* very massive stars or miniquasars, although the high efficiencies needed may point to near-zero metallicities or to a top-heavy stellar Initial Mass Function (IMF) at early times.

2 SIMULATING COSMIC REIONIZATION

In CSW we studied cosmic reionization through a combination of high-resolution N-body simulations (to describe the distribution of dark matter and diffuse gas), a semi-analytic model of galaxy formation (to track the sources of ionization) and the Monte Carlo radiative transfer code **CRASH** (to follow the propagation of ionizing photons in the IGM; Ciardi et al. 2001, CFMR; Maselli, Ferrara & Ciardi 2003). Here, we briefly summarize the features of the above approach which are relevant to the present study.

The simulations are based on a Λ CDM “concordance” cosmology with $\Omega_m=0.3$, $\Omega_\Lambda=0.7$, $h=0.7$, $\Omega_b=0.04$, $n=1$ and $\sigma_8=0.9$. These parameters are within the *WMAP* experimental error bars (Spergel et al. 2003). The re-simulation technique described in Springel et al. (2001, hereafter SWTK) and the N-body code **GADGET** (Springel, Yoshida & White 2001) were used to follow at high resolution the dark matter distribution within an approximately spherical subregion of diameter about $50h^{-1}$ Mpc within a much larger cosmological volume. Within this subregion a cube of comoving side $L = 20h^{-1}$ Mpc was used for the detailed radiative transfer modeling. The location and mass of dark matter halos was determined with a friends-of-friends algorithm. Gravitationally bound substructures were identified within the halos with the algorithm **SUBFIND** (SWTK) and were used to build the merging tree for halos and subhalos following the prescription of SWTK. The smallest resolved halos have masses of $M \simeq 10^9 M_\odot$ and they start forming in our box at $z \sim 20$. We model the galaxy population via the semi-analytic technique of Kauffmann et al. (1999) as implemented by SWTK. At the end of this process we obtain a mock catalogue of galaxies for each of the 51 simulation outputs, containing for each galaxy, among other quantities, its position, stellar mass and star formation rate. The simulations match the observed global star formation rate density evolution for $z \leq 5$. The N-body simulation used in this paper is the M3 simulation of CSW and all galaxy formation modeling is identical to that in the earlier paper.

Reionization simulations require a mass resolution high enough to follow the formation and evolution of the objects producing the bulk of the ionizing radiation. At the same time, large simulation volumes must be considered to avoid biases due to cosmic variance on small scales. Moreover, a reliable treatment of the radiative transfer of ionizing photons in the IGM is needed. So far, although several numerical approaches have been proposed (e.g. Gnedin & Ostriker 1997; CFGJ; Chiu & Ostriker 2000; Gnedin 2000; Razoumov et

<i>RUN</i>	<i>IMF</i>	f_{esc}
S5	Salpeter	5%
S20	Salpeter	20%
L20	Larson	20%

Table 1. Parameters of the simulations: Initial Mass Function, IMF; photon escape fraction, f_{esc} .

al. 2002) only the simulations described in CSW fulfill all the above requirements (refer to that paper for an extensive discussion).

One of the aims of the present study is to assess the influence of the IMF on reionization. We have thus inferred the emission properties of our model galaxies by assuming a time-dependent spectrum of a simple stellar population of metal-free stars in the mass range up to $40 M_\odot$, with two different IMFs (CFMR): (i) a Salpeter IMF and (ii) a Larson IMF, i.e. a Salpeter function at the upper mass end which falls off exponentially below a characteristic stellar mass, $M_c = 5 M_\odot$. The Larson IMF has a specific photon flux at the Lyman continuum which is about 4 times the Salpeter one. The total number of ionizing photons per solar mass for a Larson IMF is $\approx 4 \times 10^{60} M_\odot^{-1}$.

Of the emitted ionizing photons, only a fraction f_{esc} will actually be able to escape into the IGM. This quantity is poorly determined both theoretically and observationally: actually, f_{esc} may well vary with, e.g., redshift, mass and structure of a galaxy, as well as with the ionizing photon production rate (e.g. Wood & Loeb 1999; Ricotti & Shull 2000; Ciardi, Bianchi & Ferrara 2002). However, at moderate redshift, recent results on the opacity evolution of the Ly α forest (Bianchi, Cristiani & Kim 2001) constrain f_{esc} to be smaller than 20% in order not to over-produce the cosmic UV background. Although this limit may not apply to the high redshift universe, we consider this value a physically plausible upper limit.

Given these assumptions, the simulations of reionization described above have been run for the three different parameter combinations in Table 1. Run S5 (extensively described in CSW as the M3 case), yields the lowest IGM ionization power input, whereas L20 maximizes it; run S20 is an intermediate case. The critical parameter differentiating these runs is the number of ionizing photons escaping a galaxy into the IGM for each solar mass of long-lived stars which it forms. Each simulation can be thought of as corresponding to models with varying IMF, stellar luminosity beyond the Lyman limit and value of f_{esc} , provided this quantity is kept fixed (see CSW).

We quantify the agreement between our simulations and the *WMAP* data primarily through the optical depth to electron scattering, τ_e , given by:

$$\tau_e(z) = \int_0^z \sigma_T n_e(z') c \left| \frac{dt}{dz'} \right| dz', \quad (1)$$

where $\sigma_T = 6.65 \times 10^{-25} \text{ cm}^2$ is the Thomson cross section and $n_e(z')$ is the mean electron number density at z' . We will compare our simulated τ_e with the “model independent” estimate of Kogut et al. (2003) $\tau_e = 0.16 \pm 0.04$ (68% confidence range), but it should be borne in mind that the

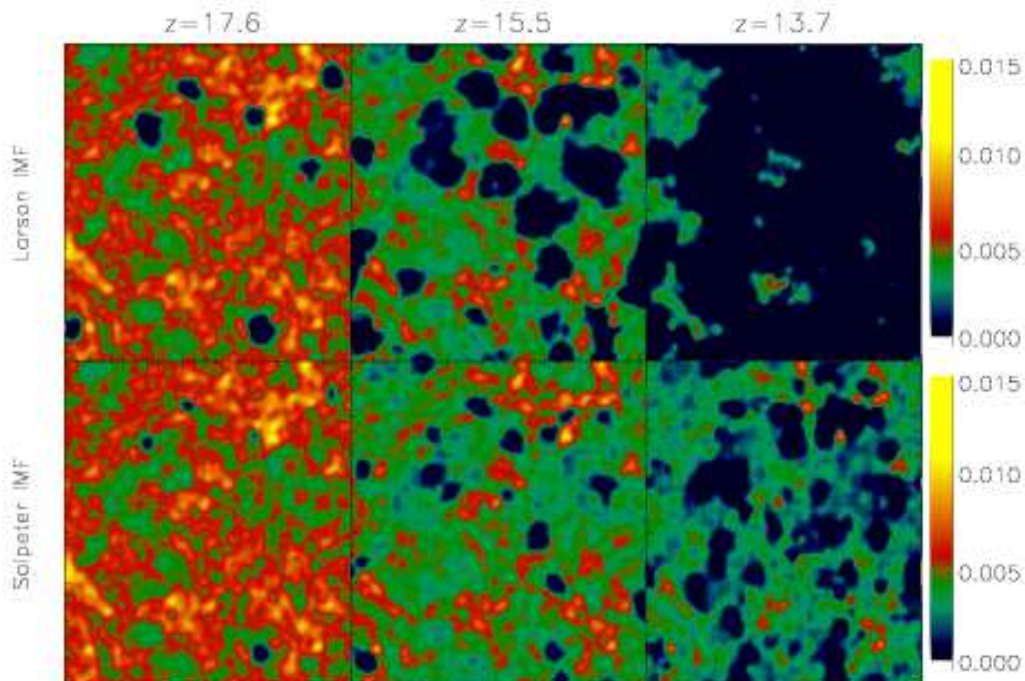


Figure 1. Slices through the simulation boxes. The six panels show the neutral hydrogen number density for the L20 (upper panels) and the S20 (lower panels) runs, at redshifts, from left to right, $z = 17.6, 15.5$ and 13.7 . The box for the radiative transfer simulation has a comoving length of $L = 20h^{-1}$ Mpc.

Spiegel et al. (2003) joint analysis of *WMAP* and external data suggests a significantly larger allowed range.

3 RESULTS

In order to clarify the differences between our runs, we start from a visual inspection of simulated maps. Fig. 1 shows the redshift evolution of the H I number density for the L20 (upper panels) and the S20 (lower) runs (illustrative maps for the S5 runs can be found in CSW). Highly ionized regions (dark areas) are produced by the young galaxies in the box and are well resolved in the maps. They initially occupy a small fraction of the volume, and are typically larger in the L20 run because of the higher ionizing power of the sources. Their shape, particularly for larger ones, appears distorted by nearby high density peaks. (To a good approximation these correspond to peaks in the H I distribution.) The ionization front slows when it encounter such overdensities because of their higher recombination rate. By redshift $z = 15.5$ several bubbles are close to overlap in the L20 run (see upper-right corner of the central panel) whereas in the S20 run the filling factor is still small. Finally, by $z = 13.7$ the overlapping fronts have cleared out most of the volume in L20 with tiny H I islands surviving thanks to their high density; reionization in the S20 run, on the other hand, is far from complete.

These remarks can be complemented by the more quantitative analysis shown in Fig. 2, which plots the (normalized) distribution function of the simulated electron density at various redshifts for the two extreme runs, L20 and S5.

This distribution is defined as the fraction of the total volume filled with gas with free electron density in each logarithmic bin of n_e . Its bimodal shape reflects the two-phase (neutral + ionized) structure of the IGM. The mean particle density in the redshift range $13.3 < z < 18.5$ is around 10^{-3} cm^{-3} , so the rightmost peak has $n_e \approx n$ and corresponds to the ionized phase. Conversely, the left peak is associated with mostly neutral gas. The general evolutionary trend is a continuous transfer of matter from the left peak to the right one as redshift decreases. By $z = 13.3$ we find that the mass-averaged neutral hydrogen fraction is only 2% for the L20 model, whereas for the S5 and S20 cases it is still 89% and 63% respectively.

The redshift evolution of the volume-averaged ionization fraction, x_v , essentially coincident with mass-averaged curve (CSW), is reported for each of our three runs in the inset of Fig. 3. An L20 vs S20 comparison shows that the former typically has an x_v value ≈ 3 times higher, reaching complete ionization ($x_v \approx 1$) at $z_r \approx 13$. Run S20, on the other hand, reaches complete reionization at $z_r \approx 11$. In run S5 reionization proceeds much more gradually and it is only at $z_r \approx 8$ that the value $x_v \approx 1$ is reached.

Finally, we have calculated the evolution of τ_e (Fig. 3) corresponding to the above reionization histories as follows. Prior to complete reionization, $n_e(z)$ in eq. 1 is obtained from the simulations; after the reionization epoch, we simply assume complete H and He I ionization throughout the box. We also assume He II reionization at $z = 3$. The three runs yield the values $\tau_e = 0.104$ (S5), $\tau_e = 0.132$ (S20) and $\tau_e = 0.161$ (L20). A value $\tau_e = 0.16$ is also obtained if

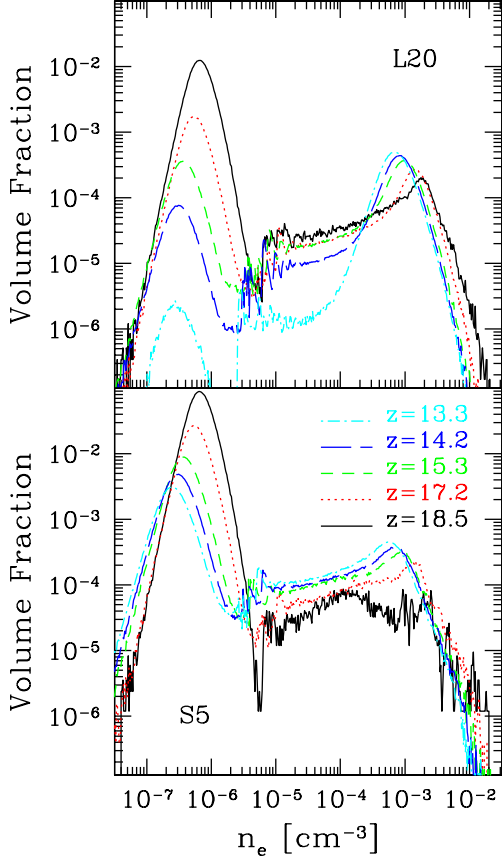


Figure 2. Evolution of the (normalized) electron density distribution function, n_e , for the L20 (upper panel) and S5 (lower panel) runs. Curves refer to different redshifts, as in the label.

one assumes instantaneous reionization at $z_r \approx 16$ (dotted line), i.e. three redshift units higher than the actual epoch of complete reionization in the model. At $z = 16$ the ionization fraction is $x_v \approx 0.3$ in L20.

4 DISCUSSION

Our supercomputer simulations of galaxy formation and of the propagation of ionization fronts have shown that recent *WMAP* measurements of the optical depth to electron scattering ($\tau_e = 0.16 \pm 0.04$ according to the “model independent” analysis of Kogut et al. (2003) or $\tau_e = 0.17 \pm 0.06$ according to the parameter fits of Spergel et al. (2003)) are easily reproduced by a model in which reionization is caused by the first stars in galaxies with total masses of a few $\times 10^9 M_\odot$. In order to get sufficient early ionization, this phase of star formation must supply a relatively high number of ionizing photons to the IGM for each solar mass of long-lived stars which is formed. This requires some combination of a high photon escape fraction, a top-heavy IMF, and a high stellar production rate for ionizing photons, similar, perhaps, to that typically inferred for metal-free stars. Among the three models we have explored, the “best” *WMAP* value for τ_e is matched assuming a moderately top-heavy IMF and an escape fraction of 20%. A Salpeter IMF with the same

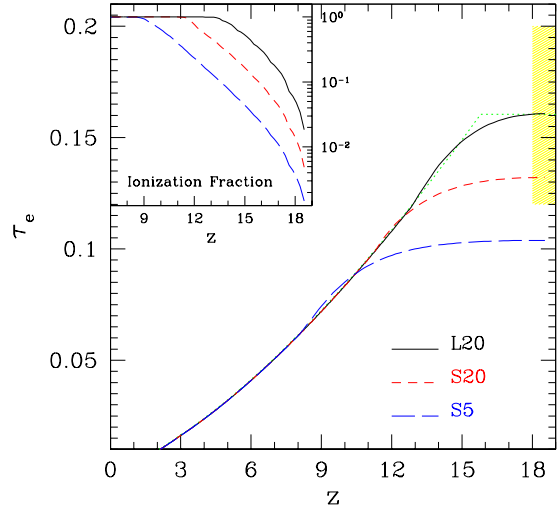


Figure 3. Redshift evolution of the electron optical depth, τ_e , for the S5 (long-dashed line), S20 (short-dashed) and L20 (solid) runs. The dotted line refers to sudden reionization at $z = 16$. The shaded region indicates the optical depth $\tau_e = 0.16 \pm 0.04$ (68% CL) implied by the Kogut et al. (2003) “model independent” analysis. In the inset the redshift evolution of the volume-averaged ionization fraction, x_v , is shown for the three runs.

escape fraction gives $\tau_e = 0.132$, which is still within all the suggested 68% confidence ranges. Decreasing f_{esc} to 5% gives $\tau_e = 0.104$, which disagrees with *WMAP* only at the 1.0 to 1.5 σ level depending on which uncertainty estimate one adopts. All these models assume that ionizing photons are produced at the level expected for metal-free stars. It is clearly possible to reproduce the experimental data without invoking exotica such as very massive stars, early “mini-quasars”, or minihalos, i.e. halos cooled by molecular hydrogen with virial temperatures $< 10^4$ K.

In our best-fitting model (L20) reionization is essentially complete by $z_r \approx 13$. This is difficult to reconcile with observations of the Gunn-Peterson effect in $z > 6$ quasars (Becker et al. 2001; Fan et al. 2002). These imply a volume-averaged neutral fraction above 10^{-3} and a mass-averaged neutral fraction $\sim 1\%$ at $z = 6$. These values are reached in our L20 run at $z \approx 13$. Even for our S5 model, they are reached before $z \approx 8$. Thus the neutral fraction at late times must be higher than in our models if the Gunn-Peterson data are to be consistent with the *WMAP* findings. A fascinating (although speculative) possibility is that the universe was reionized twice (Cen 2002; Wyithe & Loeb 2002) with a relatively short redshift interval in which the IGM became neutral again. The maximum thickness of the neutral layer (ending at $z \sim 6$) for which the L20 run remains consistent with the *WMAP* data, is $\Delta z \sim 3$; this sets the end of the first reionization epoch at $z \approx 9$. Distinguishing single- from two-epoch reionization models is in principle possible from the TE cross-correlation spectra (Naselsky & Chiang 2003); however, because of the high sensitivity required, this measurement will have to await the *Planck* mission.

What mechanism could have reduced the production of ionizing photons enough to allow recombination at the end of the first reionization epoch? Suppression of the

galaxy formation process itself seems implausible. An increase of the relevant filtering scale could have suppressed galaxy formation in halos below a typical circular velocity of $30 - 40 \text{ km s}^{-1}$ (Gnedin 2000) but this is well below the scale of the halos which host most of the star formation in our models at redshifts below 10. Feedback by SNe might reduce formation efficiencies (e.g. Madau, Ferrara & Rees 2001; Scannapieco et al. 2000) but seems likely to be more effective at the high redshifts where we need efficient star formation than at the later times when recombination is supposed to occur. A more plausible possibility may be that galaxy formation continues apace, but that the efficiency of ionizing photon production drops dramatically, perhaps as a result of increasing stellar metallicity, of decreasing escape fraction, or of changing IMF.

In many ways our models are quite conservative. We have simply extrapolated conventional models for galaxy formation to higher redshift assuming that feedback and star formation efficiencies can be scaled down to systems with mass a few $\times 10^9 M_{\odot}$ and circular velocities $\sim 60 \text{ km s}^{-1}$ at $z \approx 15$. We have adopted optimistic but not implausible values for ionizing photon production efficiency and escape fraction. We do not require any stars to form in low mass objects or through molecular cooling processes, nor do we invoke any non-stellar sources of ionizing radiation.

Processes we have ignored may nonetheless play a significant role. We do not attempt to model the possible effects of (unresolved) minihalos. Such objects rely on hydrogen molecules for cooling, and it is unclear whether they can form stars at all. As pointed out by CFGJ, and more recently by Wyithe & Loeb (2003), their contribution to the ionizing photon budget is in any case expected to be negligible. Minihalos could also increase the IGM clumping factor, thus enhancing its recombination efficiency and providing a potentially important sink for photons. If this effect were strong, more extreme assumptions about the IMF and the escape fractions would be required to ensure early reionization. One might then be forced to invoke very massive stars. For example, a $200 M_{\odot}$ star, ending its life as a pair-instability supernova ($\text{SN}_{\gamma\gamma}$), produces approximately $3 \times 10^3 (Z/Z_{\odot})$ ionizing photons/H-atom. Stars of this mass may cease to form once the metallicity of the parent gas cloud exceeds $Z \approx 10^{-5 \pm 1} Z_{\odot}$ (Bromm et al. 2001; Schneider et al. 2002). They would then disappear after they have contributed about 0.003 - 0.3 photons/H-atom, hence prior to reionization. In addition, one could posit stars outside the $\text{SN}_{\gamma\gamma}$ mass range, which end up in very massive black holes. This may lead to a star formation conundrum (Schneider et al. 2002): lacking the necessary heavy element pollution, only extremely heavy stars would form indefinitely. Although a mixture of the two populations, dominated by BH-progenitor stars might be favored by observations of the near infrared background (Salvaterra & Ferrara 2002; Magliocchetti, Salvaterra & Ferrara 2003), our current results suggest that the *WMAP* measurement of τ_e does not require any such exotic objects.

ACKNOWLEDGMENTS

We thank R. Fabbri, F. Miniati, R. Salvaterra and R. Schneider for useful discussions and in particular F. Stoehr for

collaboration during the project. This work has been partially supported by the Research and Training Network ‘‘The Physics of the Intergalactic Medium’’ set up by the European Community under the contract HPRN-CT-2000-00126. AF acknowledges ESO hospitality through the Visiting Fellowship Program.

REFERENCES

- Becker, R.H. et al. 2001, *AJ*, 122, 2850
 Bianchi, S., Cristiani, S. & Kim, T.-S. 2001, *AA*, 376, 1
 Bromm, V., Ferrara, A., Coppi, P.S. & Larson, R.B. 2001, *MNRAS*, 328, 969
 Bruscoli, M., Ferrara, A. & Scannapieco, E. 2002, *MNRAS*, 330, L43
 Cen, R. 2002, *astro-ph/0210473*
 Chiu, W. A. & Ostriker, J. P. 2000, *ApJ*, 534, 507
 Ciardi, B., Bianchi, S. & Ferrara, A. 2002, *MNRAS*, 331, 463
 Ciardi, B., Ferrara, A., Governato, F. & Jenkins, A. 2000, *MNRAS*, 314, 611 (CFGJ)
 Ciardi, B., Ferrara, A., Marri, S. & Raimondo, G. 2001, *MNRAS*, 324, 381 (CFMR)
 Ciardi, B., Stoehr, F. & White, S.D.M. 2003, *astro-ph/0301293* (CSW)
 Fan, X. et al. 2002, *AJ*, 123, 1247
 Gnedin, N. Y. 2000, *ApJ*, 535, 530
 Gnedin, N. Y. & Ostriker, J. P. 1997, *ApJ*, 486, 581
 Kauffmann, G., Colberg, J. M., Diaferio, A. & White, S. D. M. 1999, *MNRAS*, 303, 188
 Kogut, A. et al. 2003, *astro-ph/0302213*
 Madau, P., Ferrara, A. & Rees, M.J. 2001, *ApJ*, 555, 92
 Magliocchetti, M., Salvaterra, R. & Ferrara, A. 2003, *MNRAS* sub.
 Maselli, A., Ferrara, A. & Ciardi, B. 2003, *MNRAS* sub.
 Naselsky, P. & Chiang, L.-Y. 2003, *astro-ph/0302085*
 Razoumov, A. O., Norman, M. L., Abel, T. & Scott, D. 2002, *ApJ*, 572, 695
 Ricotti, M. & Shull, J. M. 2000, *ApJ*, 542, 548
 Salvaterra, R. & Ferrara, A. 2002, *astro-ph/0210331*
 Scannapieco, E., Ferrara, A. & Broadhurst, T. 2000, *ApJ*, 536, L11
 Schneider, R., Ferrara, A., Natarajan, P. & Omukai, K. 2002, *ApJ*, 571, 30
 Spergel, D.N. et al. 2003, *astro-ph/0302207*
 Springel, V., White, S. D. M., Tormen, G. & Kauffmann, G. 2001, *MNRAS*, 328, 726 (SWTK)
 Springel, V., Yoshida, N. & White, S. D. M. 2001, *NewA*, 6, 79
 Wood, K. & Loeb, A. 1999, *AAS*, 195, 1309
 Wyithe, S. & Loeb, A. 2002, *astro-ph/0209056*
 Wyithe, S. & Loeb, A. 2003, *astro-ph/0302297*